CERN – EUROPEAN ORGANIZATION FOR NUCLEAR RESEARCH

CLIC – Note – 1199

OPTIMIZATION OF THE CLIC RTML AT 380 GeV

Y. Zhao and A. Latina

CERN, Geneva, Switzerland

CERN-ACC-2024-0004
24/09/2024

Abstract

The baseline configuration of the Compact Linear Collider's Rings-to-Main-Linac section has been optimized for the 380 GeV center-of-mass energy stage, and some outstanding issues in previous designs have been resolved. In particular, the bunch compressors have been redesigned to reduce power consumption and cost. The impact of the bunch phase error from the damping ring to the ML has been investigated and optimized. A complete and improved set of beam-based alignment methods is outlined, and detailed realistic simulations showing its effectiveness in addressing static imperfections such as element misalignment and magnets strength errors are presented.

Geneva, Switzerland
24 September 2024

Optimization of the CLIC RTML at 380 GeV

Yongke Zhao* and Andrea Latina
CERN, Geneva, Switzerland

(Dated: September 24, 2024)

The baseline configuration of the Compact Linear Collider's Rings-to-Main-Linac section has been optimized for the 380 GeV center-of-mass energy stage, and some outstanding issues in previous designs have been resolved. In particular, the bunch compressors have been redesigned to reduce power consumption and cost. The impact of the bunch phase error from the damping ring to the ML has been investigated and optimized. A complete and improved set of beam-based alignment methods is outlined, and detailed realistic simulations showing its effectiveness in addressing static imperfections such as element misalignment and magnets strength errors are presented.

I. INTRODUCTION

The Ring To ML (RTML) sections of the Compact Linear Collider (CLIC) [1, 2] transport the e^- and e^+ beams from the damping ring (DR) at ground level to the main linac (ML) in the underground tunnel. A common booster linac (BL), composed of 2 GHz L-band RF structures [3], accelerates the beam from 2.86 GeV to 9 GeV. Two bunch compressors (BC1 and BC2) are used to reduce the bunch length at the end of RTML. BC1, located upstream of booster linac, is composed of the same L-band RF structures as those in the booster linac and a C-shaped chicane. BC2, located upstream of the ML, is composed of the same X-band RF structures as those in the ML and two C-shaped chicanes. The RF structures in BC1 and BC2 provide zero acceleration with a 90° off-crest phase. A spin rotator (SR) is used to provide a 90° spin rotation for the e^- beam. The beams from the booster linac are transported to the ML underground by the central arc (CA), vertical transfer line (VTL), long transfer line (LTL), and turn-around loop (TAL) sections. All arcs in the line, CA and TAL, feature a low-emittance achromatic and isochronous lattice, tightly optimized to reduce transverse emittance growth and the impact on the longitudinal plane. The schematic layout of the CLIC RTML is presented in Fig. 1.

In the CLIC Conceptual Design Report (CDR) [1] published in 2012, the RTML beamline was characterized by a high and challenging average RF gradient of 94 MV/m in the BC2 X-band RF structures. Besides, static and dynamic imperfections were not considered, which have a significant impact on the emittance growth and beam stability.

In the CLIC Project Implementation Plan (PIP) report [2] published in 2018, the bunch compressors were reoptimized for the new first energy stage at 380 GeV [4], instead of the 500 GeV in the CDR. The reoptimized BC2 average RF gradient is even higher and more challenging, which is 98.27 MV/m. The static imperfections were studied [4, 5], but to meet the emittance growth budgets at the end of RTML, the aperture of the BC2 RF structure was required to be increased by a factor of 1.5. The average iris radius of the structure was then specified as $a_0 = 5.44\,\text{mm}$ ($a_0/\lambda = 0.218$), quite large for an X-band structure, and would lead to issues such as breakdown and high cost and power consumption in RF modules.

All the outstanding issues mentioned above have been resolved, as reported in this publication, with a reoptimization of the bunch compressors and the redefinition of the beam-based alignment (BBA) strategy. In addition, the impact of the bunch phase error propagation from the DR to the ML are investigated for the first time. Our study is focused on the first stage with a center-of-mass energy of 380 GeV, with a drive beam-based acceleration in the ML.

II. BEAM PARAMETERS

The beam parameters assumed at the entrance and required at the exit of the RTML are the same as those in the CLIC PIP report, as summarized in Table I, which are common for both electrons and positrons. The budgets for the emittances at the RTML exit including imperfections are summarized in Table II. The biggest challenge comes from the static imperfections, for which 90% of machine configurations after BBA corrections must be below the emittance budgets. It has been shown in an luminosity performance report [6] that a promising luminosity can be achieved with the parameters assumed above, that with static imperfections, a luminosity of

TABLE I. Beam parameters assumed at the entrance and required at the exit of the CLIC RTML.

Parameter	Unit	Entrance	Exit
Bunches per train		352	
Particles per bunch		5.2×10^9	
Beam energy	GeV	2.86	9
Bunch length (σ_z)	μm	1800	∼70
Energy spread (σ_E/E)	%	0.12	< 1.7
Horizontal emittance ($\epsilon_{n,x}$)	nm·rad	700	< 800
Vertical emittance ($\epsilon_{n,y}$)	nm·rad	5	< 6

* yongke.zhao@cern.ch

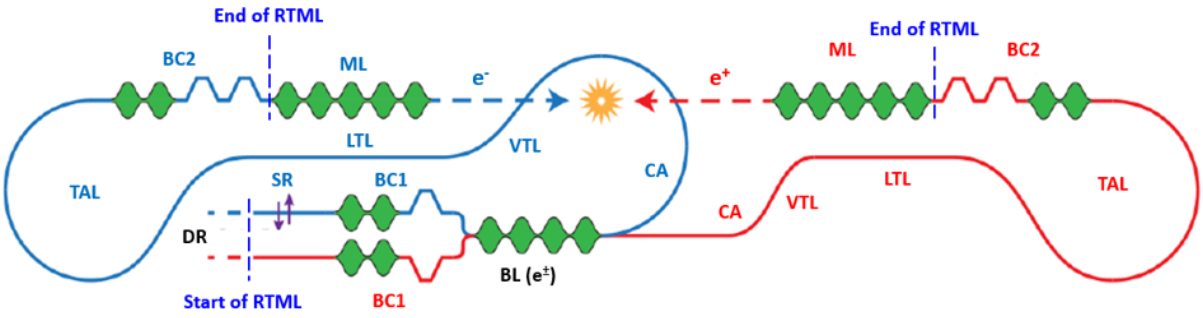

FIG. 1. Schematic layout of the CLIC RTML.

TABLE II. Emittance budgets for the CLIC RTML.

Emittance budgets	$\epsilon_{n,x}$	$\epsilon_{n,y}$
Perfect machine	< 800	< 6
Static imperfections	< 820	< 8
Static and dynamic imperfections	< 850	< 10

TABLE III. RF structure parameters used in RTML.

Parameter	Unit	"CLIC L-band"	"TD-31 X-band"
Section		BC1 & BL	BC2
RF frequency	GHz	1.999	11.994
Structure length	m	1.5	0.275
Number of cells		30	33
Phase advance per cell	°	120	120
Working RF phase	°	90	90
First iris radius	mm	20	4.062
Last iris radius	mm	14	2.6
Average iris radius	mm	17	3.331
First iris thickness	mm	8	2.525
Last iris thickness	mm	8	1.433
Average iris thickness	mm	8	1.979

$2.35 \times 10^{34}\,\mathrm{cm}^{-2}\mathrm{s}^{-1}$ or greater can be achieved by 90% of randomly misaligned machines.

III. SIMULATION AND OPTIMIZATION

Although separate bunch compressors are used for electrons and positrons, the configurations are expected to be very similar. Therefore, the bunch compressors are mainly optimized for electrons. In BC1, the same L-band RF structure is used as that in the booster linac (BL), which is called the "CLIC L-band" structure. The BC2 uses the same "TD-31 X-band" RF structure that is used in the ML. The structure parameters are summarized in Table III.

Simulations are performed with *Placet* [7], with collective effects taken into account, such as short-range wakefield, incoherent synchrotron radiation (ISR) and coherent synchrotron radiation (CSR) effects. In the optimization, *RF-Track* [8] is also used for quick and simplified simulations.

TABLE IV. Klystron parameters assumed in optimization for different RF structures.

Parameter	Unit	"CLIC L-band"	"TD-31 X-band"
Section		BC1 & BL	BC2
Output power	MW	50	51.4
Pulse length	μs	8	2

To optimize the cost of the RF modules, certain assumptions have been made in the RF system. Similar klystrons and pulse compressors as those used in the CLIC PIP report are assumed in the optimization. The parameters of the klystrons are summarized in Table IV. The power gains as a function of the compression factors are presented in Fig. 2, which are obtained from interpolations of the data in the CLIC PIP report. The schematic layout of the RF module is presented in Fig. 3, where the number of structures per RF module is 4 for the "CLIC L-band" and 8 for the "TD-31 X-band", same as those used in the CLIC PIP report. A total RF transmission efficiency of 90% is always assumed. The cost analysis uses arbitrary cost units set to:

- Klystron cost: 300 a.u. each
- RF structure cost: 50 a.u. per meter

The *CLICopti* [9] tool is used to estimate the RF performance, such as the input power, pulse length and structure breakdown. The breakdown rate standard used in the estimation is 10^{-6} breakdowns/pulse/meter. In this work, the beam loading effect is considered only for the booster linac, where the RF phase is on-crest.

A start-to-end optimization involves optimizing the RF gradient and the number of structures, aiming to reduce the total cost while meeting the bunch parameter requirements at the RTML exit. The two chicanes in BC2 are required to have the same bending angle to reduce the ISR and CSR effects on the emittance growth and simplify the optimization. In addition, the matching quadrupoles between different sections are also reoptimized to minimize

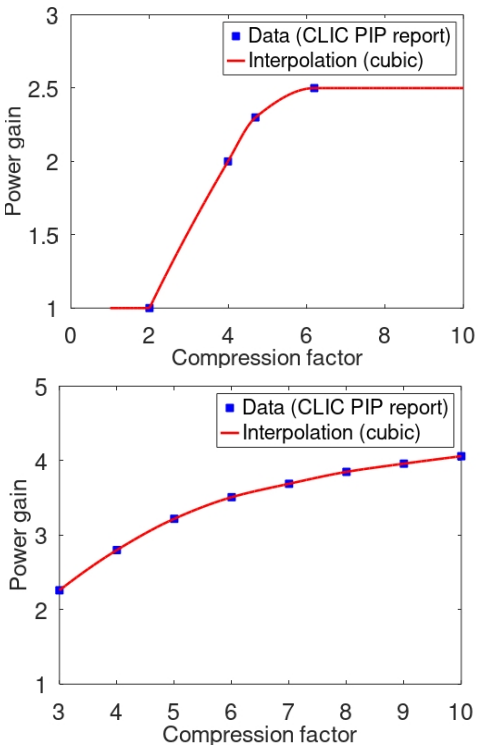

FIG. 2. Power gain as a function of compression factor for the pulse compressors assumed for the "CLIC L-band" (top plot) and the "TD-31 X-band" (bottom plot) structures.

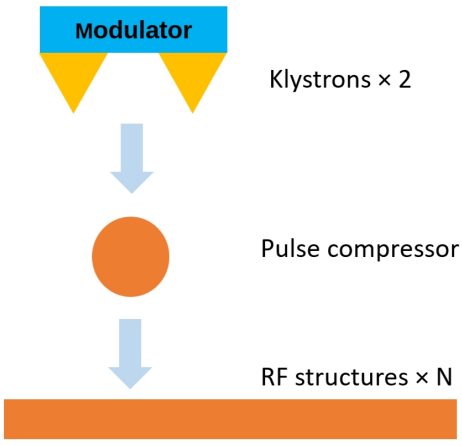

FIG. 3. Schematic layout of RF module.

the emittance growth. The optimized parameters and results are compared with the old parameters and results, as summarized in Table V, for the electron beam. The optimization significantly reduces the average structure aperture and gradient, total voltage, number of structures and expected cost in BC2 RF section, and the emittance growth in RTML. The average structure iris radius in BC2 RF section is reduced from 5.44 mm to 3.33 mm by 39%. The average BC2 RF gradient is reduced from 98.27 MV/m to 74.916 MV/m by 24%. The total BC2 RF voltage is reduced from 1763.0 MV to 659.3 MV by 63%. The number of BC2 RF structures is reduced from 78 to 32 by 59%, though the structure length is increased by 20%. The expected cost of structures and klystrons is reduced by 20% in BC1, 1.4% in BL and 78% in BC2. The normalized emittance growth is reduced by 14% horizontally and 43% vertically. It is found that the same configuration of the bunch compressors and booster linac can be used for the positrons.

TABLE V. Comparison between the old and optimized parameters and results in RTML for electrons.

Parameter	Unit	Old	New
BC1 RF total voltage	MV	477	450.5
BC1 bending angle	°	4.42	3.95
BC1 structure length	m	1.5	1.5
BC1 RF gradient	MV/m	15.9	18.770
BC1 RF peak power	MW	34.0	47.3
BC1 RF-to-beam efficiency	%	22.9	20.8
BC1 number of klystrons		10	8
BC1 number of RF structures		20	16
BC1 expected RF cost	a.u.	4500	3600
BL total voltage	MV	6168.6	6156.3
BL structure length	m	1.5	1.5
BL RF gradient	MV/m	14.9	15.089
BL RF peak power	MW	54.1	55.1
BL RF-to-beam efficiency	%	20.0	19.9
BL number of klystrons		138	136
BL number of RF structures		276	272
BL expected RF cost	a.u.	62100	61200
BC2 RF total voltage	MV	1763.0	659.3
BC2 bending angles	°	1.56, 0.10	1.55, 1.55
BC2 structure length	m	0.23	0.275
BC2 structure aperture	mm	5.44	3.33
BC2 RF gradient	MV/m	98.27	74.916
BC2 RF peak power	MW	355.6	39.3
BC2 RF-to-beam efficiency	%	7.5	45.1
BC2 number of klystrons		156	8
BC2 number of RF structures		78	32
BC2 expected RF cost	a.u.	47700	2840
Bunch length at BC1 exit	μm	235	410
Final bunch length	μm	70	70
Final energy spread (σ_E/E)	%	1.0	1.1
Hori. emittance growth ($\Delta\epsilon_{n,x}$)	nm·rad	86	74
Vert. emittance growth ($\Delta\epsilon_{n,y}$)	nm·rad	0.7	0.4

IV. NOMINAL PERFORMANCE

The simulation results at the RTML exit for a perfect machine without any imperfections are summarized in Table VI, for both electrons and positrons. The emittance growth along the RTML beamline is presented in Fig. 4. The longitudinal phase space at the RTML exit is presented in Fig. 5, where a full bunch compression is achieved.

TABLE VI. Simulation results at RTML exit for a perfect machine.

Parameter	Unit	e^-	e^+
Bunch length (σ_z)	μm	70.4	68.6
Energy spread (σ_E/E)	%	1.07	1.08
Horizontal emittance ($\epsilon_{n,x}$)	nm·rad	773.8	763.1
Vertical emittance ($\epsilon_{n,y}$)	nm·rad	5.40	5.08

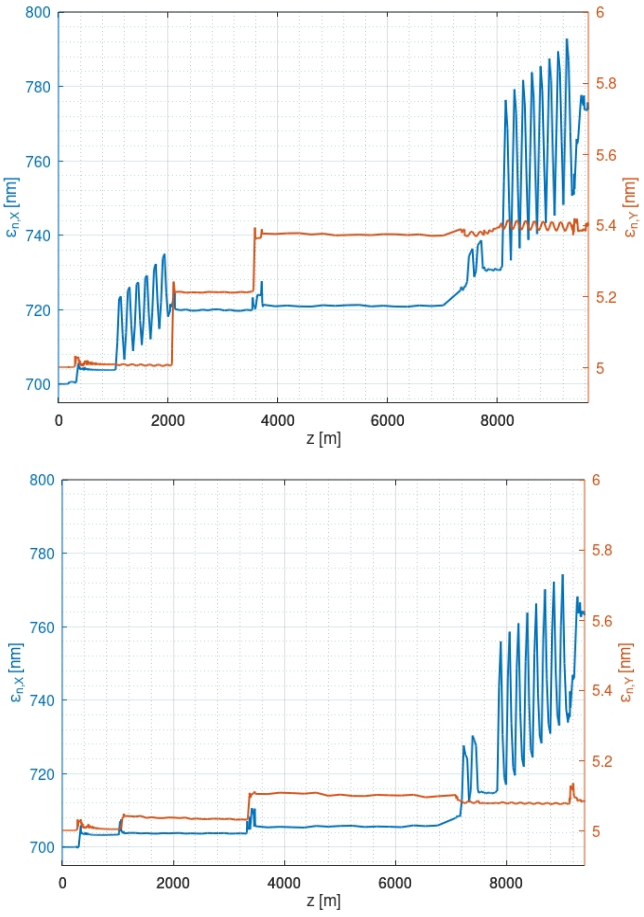

FIG. 4. Emittance growth along the RTML beamline for electron (top) and positron lines (bottom).

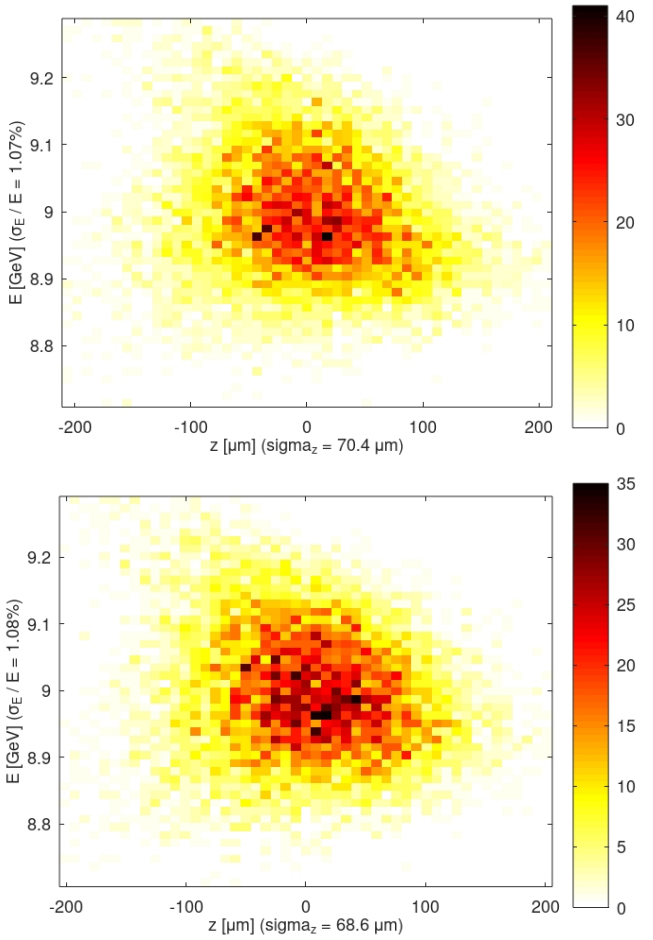

FIG. 5. Longitudinal phase space at the RTML exit for electron bunch (top) and positron bunch (bottom).

TABLE VII. Static imperfections considered in the study, with the RMS values reported.

Imperfection	Unit	Value
Magnet and BPM positron error	μm	30
Magnet and BPM tilt error	μrad	100
Magnet and BPM roll error	μrad	100
Quadrupole strength error in CA & TAL	%	0.01
Quadrupole strength error in other sections	%	0.1
Other magnet strength error	%	0.1
BPM resolution	μm	1
Magnetic center shift w/ strength scaling	μm / 5%	0.35
Emittance measurement uncertainty	%	1

V. IMPERFECTIONS

A. Static imperfections

The static imperfections considered in the study are summarized in Table VII, with the RMS values reported.

Similar beam-based alignment (BBA) methods as those used in [10] are used for the corrections of static imperfections and are summarized as follows:

- One-to-one (OTO) correction: An orbit correction method using dipole kickers as the correctors. Each dipole corrector is placed downstream of a beam position monitor (BPM) and a quadrupole. The strengths of the dipole correctors are adjusted such that the beam is steered through the centers of the BPMs to avoid beam loss. The dipole strengths are estimated by minimizing the offset of the trajectory in BPM, which is equivalent to solving the following

equations:

$$\begin{pmatrix} -\mathbf{x} \\ \mathbf{0} \end{pmatrix} = \begin{pmatrix} \mathbf{R} \\ \beta_0 \mathbf{I} \end{pmatrix} \cdot \begin{pmatrix} \theta_{\mathbf{1}} \\ \vdots \\ \theta_{\mathbf{m}} \end{pmatrix} , \tag{1}$$

where $\mathbf{x}$ represents the BPM readings, $\mathbf{R}$ is the orbit response matrix and $\theta_{\mathbf{1},\ldots,\mathbf{m}}$ represents the dipole corrections. $\mathbf{0}$ and $\mathbf{I}$ are zero and identity matrices. β_0 is a regulatory and free parameter to constrain the corrections and to condition the system, which is usually empirically chosen.

- Dispersion-free steering (DFS) correction: An orbit and dispersion correction method using the same dipole correctors as the OTO correction. The dispersion is measured with an off-energy test beam and corrected by minimizing the difference between the nominal and dispersive trajectories in BPM, which is equivalent to solving the following equations:

$$\begin{pmatrix} & -\mathbf{x} & \\ \omega_d & (\eta_{\mathbf{0}} - \eta) & \\ & \mathbf{0} & \end{pmatrix} = \begin{pmatrix} & \mathbf{R} & \\ \omega_d & \mathbf{D} & \\ \beta_1 & \mathbf{I} & \end{pmatrix} \cdot \begin{pmatrix} \theta_{\mathbf{1}} \\ \vdots \\ \theta_{\mathbf{m}} \end{pmatrix} , \tag{2}$$

where, in addition to the OTO correction, η and $\eta_{\mathbf{0}}$ are the measured and target dispersions, and $\mathbf{D}$ is the dispersion response matrix. ω_d is a weighting factor to constrain the dispersion correction, which is also usually chosen empirically for better performance, though it can be estimated theoretically from the following formula:

$$\omega_d^2 = \frac{\sigma_{\text{pos}}^2 + \sigma_b^2}{2\sigma_b^2} , \tag{3}$$

where σ_{pos} and σ_b are the BPM misalignment and resolution. The test beam for the dispersion measurement is obtained by scaling the strengths of all the magnets, corresponding to a reduction of 5% in the beam energy. However, an additional misalignment of the magnets is introduced, as reported in Table VII.

- Sextupole-based emittance tuning (SBET) correction: An emittance optimization method using sextupoles as correctors. The positions of the sextupole correctors are adjusted such that the measured emittances at the end of the corrected lattice are minimized. A 1% RMS uncertainty is assumed for the emittance measurements which is the same as the one used in previous studies [4, 5]. The first 5 sextupoles of the sections in the correction are used as correctors. The Simplex algorithm [11] is used to search for the optimal parameters, with a merit function defined as follows:

$$\text{Merit} = \sqrt{\left(\frac{\epsilon_x - \epsilon_x^0}{\epsilon_x^1 - \epsilon_x^0}\right)^2 + \left(\frac{\epsilon_y - \epsilon_y^0}{\epsilon_y^1 - \epsilon_y^0}\right)^2} , \tag{4}$$

where $\epsilon_{x,y}$ is the horizontal or vertical emittance from the measurements, $\epsilon_{x,y}^0$ is the initial emittance at the RTML entrance, as reported in Table I, and $\epsilon_{x,y}^1$ is the emittance budget for static imperfections, as reported in Table II.

TABLE VIII. Common BBA parameters.

Parameter	Value
β_0	1
β_1	1
ω_d	30
Number of quadrupoles per bin	40
Bin overlap	50%
Number of iterations in OTO correction	3
Number of iterations in DFS correction	3

The OTO and DFS corrections are applied to the RTML beamline section by section, with a small overlap between the neighbouring sections. Each section is split into subsections or bins. All bins in a secton have equal number of quadrupoles and there is an overlap between the neighbouring bins. In each bin, the corrections are applied in several iterations. The TAL section is split into two smaller sections, TAL1 and TAL2, in the corrections to avoid beam loss. The BBA parameters mentioned above are summarized in Table VIII, which are commonly used in all sections.

The BBA correction procedure is implemented in steps, as summarized in Table IX. The study is focused on the corrections for the electron beam, with 100 randomly misaligned machines simulated. For the positron beam, the corrections are thought to be much easier, given that the emittance growth is much smaller. As a result of the BBA corrections, the emittances of 99% corrected machines are below the emittance budget at the RTML exit, which meets well the requirement of $\geq 90\%$, as presented in Fig. 6.

TABLE IX. BBA correction procedure in steps.

Step	Sections	Corrections
1	SR–LTL	OTO & DFS
2	CA–LTL	SBET
3	TAL–BC2	OTO & DFS
4	TAL–BC2	SBET

B. Bunch phase error

The impact of the bunch phase error propagation from the DR to the ML is also studied and presented in Fig. 7. The tolerance for the bunch phase error at the ML entrance is assumed to be $\pm 0.1^\circ$ [1] in the plot, giving an acceptance at the DR exit of 5°, which is thought to be quite satisfied, as the required minimum acceptance is 2.5° [1].

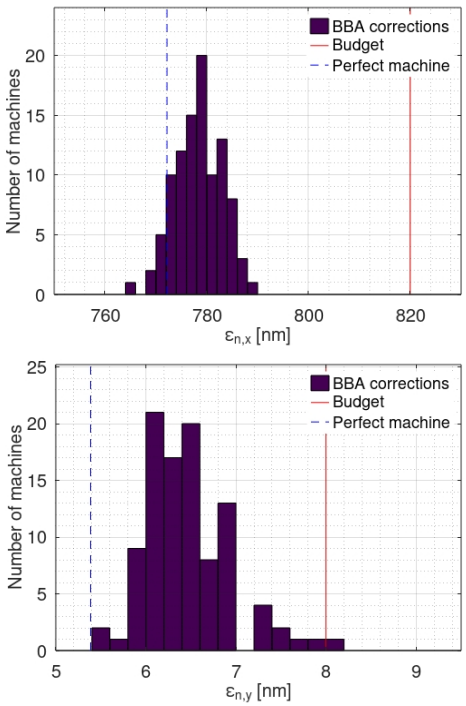

FIG. 6. Horizontal (top plot) and vertical (bottom plot) emittances after BBA corrections at the RTML exit for the electron beam.

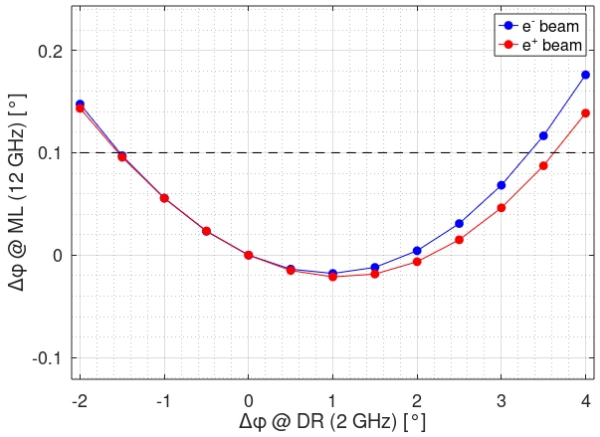

FIG. 7. Impact of bunch phase error ($\Delta\varphi$) propagation from the DR to the ML.

VI. CONCLUSIONS

We present an optimization of the CLIC RTML beamline for the first stage of CLIC, focusing mainly on the bunch compressors and matching sections. The optimization significantly reduces the average structure aperture and gradient, total voltage, number of structures and expected cost in BC2 RF section, and the emittance growth throughout the entire system. The average structure iris radius in BC2 RF section is reduced from 5.44 mm to 3.33 mm. The average BC2 RF gradient is reduced from 98.27 MV/m to 74.916 MV/m. The number of BC2 RF structures is reduced from 78 to 32, though the structure length is increased by 20%. The expected cost of structures and klystrons is reduced by 20% in BC1, 1.4% in BL and 78% in BC2. The normalized emittance growth is reduced by 14% horizontally and 43% vertically. With an updated beam-based alignment correction procedure, tight emittance growth requirements have been achieved with 99% of randomly misaligned machines under the effects of static imperfections, satisfying well the budgets. The bunch phase error propagation from the DR to the ML have also been studied, and a result within the acceptance at the DR exit has been found.

ACKNOWLEDGMENTS

The authors thank C. Gohil, Y. Han and X. Liu for their contributions to the previous development of the simulation framework. The authors also thank J. Olivares, P. Wang, A. Grudiev, D. Schulte, Y. Papaphilippou and H. Bartosik for the helpful discussions and suggestions.

[1] M. Aicheler, P. Burrows, M. Draper, T. Garvey, P. Lebrun, K. Peach, N. Phinney, H. Schmickler, D. Schulte, and N. Toge, *A Multi-TeV Linear Collider Based on CLIC Technology: CLIC Conceptual Design Report*, CERN Yellow Reports: Monographs (CERN, Geneva, 2012).

[2] M. Aicheler, P. Burrows, N. Catalan Lasheras, R. Corsini, M. Draper, J. Osborne, D. Schulte, S. Stapnes, and M. Stuart (CLICAccelerator), *The Compact Linear Collider (CLIC) – Project Implementation Plan*, edited by M. Aicheler, CERN Yellow Reports: Monographs (2018) 247 p.

[3] E. Darvish Roknabadi and S. Döbert, *TW-Structure Design and E-Field Study for CLIC Booster Linac*, Tech. Rep. (2016).

[4] Y. Han, A. Latina, L. Ma, and D. Schulte, *Beam-Based Alignment for the Rebaselining of CLIC RTML*, Tech. Rep. (2017).

[5] Y. Han, A. Latina, L. Ma, and D. Schulte, Static beam-based alignment for the Ring-To-Main-Linac of the Compact Linear Collider, JINST **12** (06), P06010.

[6] C. Gohil, P. N. Burrows, N. Blaskovic Kraljevic, A. Latina, J. Ögren, and D. Schulte, Luminosity performance of the compact linear collider at 380 gev with static and dynamic imperfections, Phys. Rev. Accel. Beams **23**, 101001 (2020).

[7] A. Latina, Y. Levinsen, D. Schulte, and J. Snuverink, Evolution of the Tracking Code PLACET, in *4th International Particle Accelerator Conference* (2013) p. MOPWO053.

[8] A. Latina, Update of the Tracking Code RF-Track, JACoW **IPAC 2021**, 4180 (2021).

[9] K. N. Sjobak and A. Grudiev, *The CLICopti RF structure parameter estimator*, Tech. Rep. (CERN, Geneva, 2014).

[10] A. Latina, J. Pfingstner, D. Schulte, E. Adli, F. J. Decker, and N. Lipkowitz, Experimental demonstration of a global dispersion-free steering correction at the new linac test facility at slac, Phys. Rev. ST Accel. Beams **17**, 042803 (2014).

[11] J. A. Nelder and R. Mead, A Simplex Method for Function Minimization, The Computer Journal **7**, 308 (1965), https://academic.oup.com/comjnl/article-pdf/7/4/308/1013182/7-4-308.pdf.